

EMPIRICAL FORMULA FOR DESIGNING SYMMETRIC/ANTI-SYMMETRIC FIR SINGLE BAND PCLS FILTERS

Charlotte Yuk-Fan Ho¹, Bingo Wing-Kuen Ling², Zhi-Wei Chi², Chi-Wah Kok³, Wan-Chi Siu³

School of Mathematical Science, Queen Mary College, University of London¹

Department of Electronic Engineering, Division of Engineering, King's College London²

Department of Electronic and Information Engineering, Hong Kong Polytechnic University³

ABSTRACT

An empirical formulation that relates the filter length, the transition bandwidth, the cutoff frequency, the maximum passband ripple magnitude, the maximum stopband ripple magnitude and the total ripple energy of symmetric/anti-symmetric finite impulse response (FIR) single band peak constrained least squares (PCLS) filters is presented. Design examples are presented to demonstrate the application and accuracy of the presented formula.

1. INTRODUCTION

The peak constrained least squares (PCLS) filters [1-2] have been shown to be able to achieve high design flexibility that allows the tradeoff between the total ripple energy, the maximum passband ripple magnitude and the maximum stopband ripple magnitude. However, the filter length, the transition bandwidth, the cutoff frequency, the maximum passband ripple magnitude and the maximum stopband ripple magnitude are usually required to be specified for the filter design problem. An empirical formula that relates the above design parameters is useful for determining the design specification to meet a certain application. Similar problems for symmetric/anti-symmetric FIR single band minimax filters have been considered in [3-4]. Even though the minimax filter is a degenerated PCLS filter with the maximum passband ripple magnitude and the maximum stopband ripple magnitude constrained to be the smallest achievable values for the given filter specification, the empirical formulas presented in [3-4] cannot be applied to the design of PCLS filter. This is because the total ripple energy of the filter is not considered. In this paper, an empirical formula that relates all the necessary design parameters of a PCLS filter is presented.

2. PCLS FILTER DESIGN FORMULATION

Let $H_0(\omega)$ and $D(\omega)$ denote the magnitude response of a length N symmetric/anti-symmetric FIR single band PCLS filter, and the desired magnitude response, respectively. Let the length N vector \mathbf{x} be the filter coefficient vector of $H_0(z)$, such that $H_0(\omega) = (\eta(\omega))^T \mathbf{x}$ with an appropriate sine or cosine vector $\eta(\omega)$, and the superscript T denotes the transposition operator. Denote $f_c, \Delta B, B_p, B_s, \delta_p, \delta_s$ and $J(\delta_p, \delta_s, f_c, \Delta B, N)$ as the center frequency, the transition bandwidth, the passband, the stopband, the maximum passband ripple magnitude, the maximum stopband ripple magnitude, and the total ripple energy of the filter respectively. As a result,

$$J(\delta_p, \delta_s, \Delta B, N) = \int_{B_p \cup B_s} W(\omega) |H_0(\omega) - D(\omega)|^2 d\omega, \quad (1)$$

where $W(\omega)$ is the weighting function in which $W(\omega) > 0 \forall \omega \in B_p \cup B_s$. Denote

$$\mathbf{Q}(f_c, \Delta B, N) \equiv 2 \int_{B_p \cup B_s} W(\omega) \eta(\omega) (\eta(\omega))^T d\omega, \quad (2)$$

$$\mathbf{b}(f_c, \Delta B, N) \equiv -2 \int_{B_p \cup B_s} W(\omega) D(\omega) \eta(\omega) d\omega, \quad (3)$$

$$p(f_c, \Delta) \equiv \int_{B_p \cup B_s} W(\omega) (D(\omega))^2 d\omega. \quad (4)$$

Then

$$J(\delta_p, \delta_s, f_c, \Delta B, N) = \frac{1}{2} \mathbf{x}^T \mathbf{Q}(f_c, \Delta B, N) \mathbf{x} + (\mathbf{b}(f_c, \Delta B, N))^T \mathbf{x} + p(f_c, \Delta B). \quad (5)$$

Given a set of design specifications $f_c, \Delta B, N, D(\omega)$ and $W(\omega)$ for $H_0(z)$, the cost functions $\mathbf{Q}(f_c, \Delta B, N)$, $\mathbf{b}(f_c, \Delta B, N)$ and $p(f_c, \Delta B)$ can be evaluated analytically. Consequently, the PCLS filter design problem can be formulated as the following optimization problem.

$$\begin{aligned} \min_{\mathbf{x}} J(\delta_p, \delta_s, f_c, \Delta B, N) &= \frac{1}{2} \mathbf{x}^T \mathbf{Q}(f_c, \Delta B, N) \mathbf{x} \\ &+ (\mathbf{b}(f_c, \Delta B, N))^T \mathbf{x} + p(f_c, \Delta B). \quad (6) \\ \text{subject to } |(\eta(\omega))^T \mathbf{x} - D(\omega)| &\leq \delta_p, \quad \forall \omega \in B_p, \\ \text{and } |(\eta(\omega))^T \mathbf{x} - D(\omega)| &\leq \delta_s, \quad \forall \omega \in B_s. \end{aligned}$$

3. EMPIRICAL FORMULA

In order to determine an empirical formula for symmetric/antisymmetric FIR single band PCLS filter, a large amount of PCLS designs are considered for the following five sets of design specifications presented in subsequent sections. All the filters are designed with $W(\omega) = 1 \forall \omega \in B_p \cup B_s$ and a brickwall desired filter

$$D(\omega), \text{ such that } D(\omega) = \begin{cases} 1 & \forall \omega \in B_p \\ 0 & \forall \omega \in B_s \end{cases}. \text{ The filter specification}$$

parameters extracted from the obtained filters will then be used to formulate the empirical formula.

3.1 Filter Length vs Total Ripple Energy

Filters with various filter lengths are designed subject to fixed values of the maximum passband ripple magnitude, the maximum stopband ripple magnitude, the center frequency and the transition bandwidth. Other design parameters are $\delta_p = \delta_s = 0.002$, $f_c = \frac{\pi}{2}$, and $\Delta B = 0.08\pi$. Fig 1(a) shows a plot of the total ripple energy against the filter length. It can be seen from Fig 1(a) that there is a linear relationship between the total ripple energy in dB and the filter length.

$$10 \log_{10} J(\delta_p, \delta_s, f_c, \Delta B, N) = a_{1,1}(f_c, \Delta B, \delta_p, \delta_s) N + a_{1,2}(f_c, \Delta B, \delta_p, \delta_s), \quad (7)$$

where $a_{1,1}(\dots)$ and $a_{1,2}(\dots)$ are the corresponding slope and the intercept of the straight line in Fig 1(a), respectively.

3.2 Transition Bandwidth vs Total Ripple Energy

Filters with various transition bandwidths are designed subject to fixed values of the maximum passband ripple magnitude, the maximum stopband ripple magnitude, the center frequency, the transition bandwidth and the filter length. Other design parameters are $\delta_p = \delta_s = 0.01$, $f_c = \frac{\pi}{2}$, and $N = 30$. Fig 1(b) shows a plot of the total ripple energy against the transition bandwidth. It can be seen

from Fig 1(b) that there is a linear relationship between the total ripple energy in dB and the transition bandwidth.

$$10\log_{10}J(\delta_p, \delta_s, f_c, \Delta B, N) = a_{2,1}(f_c, \Delta B, \delta_p, \delta_s)\Delta B + a_{2,2}(f_c, \Delta B, \delta_p, \delta_s), \quad (8)$$

where $a_{2,1}(\dots)$ and $a_{2,2}(\dots)$ are the corresponding slope and the intercept of the straight line in Fig 1(b), respectively.

3.3 Maximum Passband Ripple Magnitude vs Total Ripple Energy

Filters with various maximum passband ripple magnitudes are designed subject to fixed values of the maximum stopband ripple magnitude, the center frequency, the transition bandwidth and the filter length. Other design parameters are $\delta_s = 0.01$, $f_c = \frac{\pi}{2}$, $\Delta B = 0.08\pi$ and $N = 30$. Fig. 1(c) shows a plot of the total ripple energy against the maximum passband ripple magnitude. It can be seen from Fig. 1(c) that there is a convex downsloping relationship between the total ripple energy in dB and the maximum passband ripple magnitude in dB. This property of the PCLS filter has been described in [5]. In order to quantitatively describe the relationship between the total ripple energy and the maximum passband ripple magnitude, a polynomial approximation with order M_p is proposed.

$$10\log_{10}J(\delta_p, \delta_s, f_c, \Delta B, N) = \sum_{k=0}^{M_p} a_{3,k}(f_c, \Delta B, N, \delta_s)(20\log_{10} \delta_p)^k. \quad (9)$$

The squares error of the approximation is given by

$$E_p(\delta_p, M_p) = \left(\sum_{k=0}^{M_p} a_{3,k}(f_c, \Delta B, N, \delta_s)(20\log_{10} \delta_p)^k - 10\log_{10}J(\delta_p, \delta_s, f_c, \Delta B, N) \right)^2. \quad (10)$$

Fig 2(a) plots $E_p(\delta_p, M_p)$ against M_p and δ_p for the simulation results in Fig 1(c). It can be seen from Fig 2(a) that the squares error is smaller than 0.0012 when $M_p \geq 5$. Hence, a fifth order polynomial is good enough for the approximation.

3.4 Maximum Stopband Ripple Magnitude vs Total Ripple Energy

Filters with various maximum stopband ripple magnitudes are designed subject to fixed values of the maximum passband ripple magnitude, the center frequency, the transition bandwidth and the filter length. Other design parameters are $\delta_p = 0.01$, $f_c = \frac{\pi}{2}$, $\Delta B = 0.08\pi$ and $N = 30$. Fig 2(b) shows a plot of the total ripple energy against the maximum stopband ripple magnitude. It can be seen from Fig 2(b) that the total ripple energy in dB and the maximum stopband ripple magnitude in dB is also convex downsloping related. This property is also described in [5]. In order to quantitatively describe the relationship between the total ripple energy and the maximum stopband ripple magnitude, a polynomial approximation with order M_s is proposed.

$$10\log_{10}J(\delta_p, \delta_s, f_c, \Delta B, N) = \sum_{k=0}^{M_s} a_{4,k}(f_c, \Delta B, N, \delta_p)(20\log_{10} \delta_s)^k. \quad (11)$$

The squares error of the approximation is given by

$$E_s(\delta_s, M_s) = \left(\sum_{k=0}^{M_s} a_{4,k}(f_c, \Delta B, N, \delta_p)(20\log_{10} \delta_s)^k - 10\log_{10}J(\delta_p, \delta_s, f_c, \Delta B, N) \right)^2. \quad (12)$$

Fig 2(c) plots $E_s(\delta_s, M_s)$ against M_s and δ_s of the simulation results in Fig 2(b). It can be seen from Fig 2(c) that the squares error is smaller than 0.0051 when $M_s \geq 5$. Hence, a fifth order polynomial is good enough for the approximation.

3.5 Center Frequency vs Total Ripple Energy

Filters with various center frequencies are designed subject to fixed values of the maximum passband ripple magnitude, the maximum stopband ripple magnitude, the transition bandwidth and the filter length. Other design parameters are $\delta_p = \delta_s = 0.01$, $\Delta B = 0.08\pi$ and $N = 30$. Fig 3(a) shows a plot of the total ripple energy in dB against the center frequency. It can be seen from Fig 3(a) that there is a sinusoidal relationship between the total ripple energy and the center frequency. In order to quantitatively describe the relationship between the total ripple energy and the center frequency, a sinusoidal approximation with amplitude $A_f(\Delta B, N, \delta_p, \delta_s)$, phase shift $\phi_f(\Delta B, N, \delta_p, \delta_s)$, DC offset $c_f(\Delta B, N, \delta_p, \delta_s)$ and frequency $\hat{\omega}_f(\Delta B, N, \delta_p, \delta_s)$ is employed to model the total ripple energy

$$10\log_{10}J(\delta_p, \delta_s, f_c, \Delta B, N) = A_f(\Delta B, N, \delta_p, \delta_s)(\sin(\hat{\omega}_f(\Delta B, N, \delta_p, \delta_s)f_c + \phi_f(\Delta B, N, \delta_p, \delta_s))) + c_f(\Delta B, N, \delta_p, \delta_s). \quad (13)$$

The squares error of the approximation is given by

$$E_f(f_c) = (A_f(\Delta B, N, \delta_p, \delta_s)(\sin(\hat{\omega}_f(\Delta B, N, \delta_p, \delta_s)f_c + \phi_f(\Delta B, N, \delta_p, \delta_s))) + c_f(\Delta B, N, \delta_p, \delta_s) - 10\log_{10}J(\delta_p, \delta_s, f_c, \Delta B, N))^2. \quad (14)$$

Fig 3(b) plots $E_f(f_c)$ against f_c for the simulation results in Fig 3(a). It can be seen from Fig 3(b) that the squares error is smaller than 0.0113, which is good enough for most filter design applications.

An empirical formula relating the filter length, the transition bandwidth, the cutoff frequency, the maximum passband ripple magnitude, the maximum stopband ripple magnitude and the total ripple energy of a symmetric/anti-symmetric FIR single band PCLS filter can now be formulated by combining the above individual models.

$$10\log_{10}J(\delta_p, \delta_s, f_c, \Delta B, N) = (\hat{A}_f \sin(\hat{\omega}_f f_c + \phi_f) + 1) \times \sum_{m=0}^{M_p} \sum_{n=0}^{M_s} (a_{m,n}^1 N \Delta B + a_{m,n}^2 N + a_{m,n}^3 \Delta B + a_{m,n}^4) \times (20\log_{10} \delta_p)^m (20\log_{10} \delta_s)^n, \quad (15)$$

where \hat{A}_f , $\hat{\omega}_f$, ϕ_f , and $a_{m,n}^k$ for $k = 1, 2, 3, 4$, $m = 0, 1, \dots, M_p$ and $n = 0, 1, \dots, M_s$ are constant parameters independent of N , f_c , ΔB , δ_p and δ_s .

3.6 Estimation of Parameters

Note that $\hat{\omega}_f$ and ϕ_f can be estimated directly from Fig 3(a). To estimate other parameters in the proposed model, define

$$\mathbf{a} = \begin{bmatrix} a_{0,0}^1 & \cdots & a_{0,M_s}^1 & \cdots & a_{M_p,0}^1 & \cdots & a_{M_p,M_s}^1 & \cdots \\ \cdots & a_{0,0}^4 & \cdots & a_{0,M_s}^4 & \cdots & a_{M_p,0}^4 & \cdots & a_{M_p,M_s}^4 \end{bmatrix}^T$$

and

$$\mathbf{M}(N, \Delta B, \delta_p, \delta_s) = \begin{bmatrix} N\Delta B(20\log_{10}\delta_p)^0(20\log_{10}\delta_s)^0 \\ \vdots \\ N\Delta B(20\log_{10}\delta_p)^0(20\log_{10}\delta_s)^{M_s} \\ \vdots \\ N\Delta B(20\log_{10}\delta_p)^{M_p}(20\log_{10}\delta_s)^0 \\ \vdots \\ N\Delta B(20\log_{10}\delta_p)^{M_p}(20\log_{10}\delta_s)^{M_s} \\ \vdots \\ (20\log_{10}\delta_p)^0(20\log_{10}\delta_s)^0 \\ \vdots \\ (20\log_{10}\delta_p)^0(20\log_{10}\delta_s)^{M_s} \\ \vdots \\ (20\log_{10}\delta_p)^{M_p}(20\log_{10}\delta_s)^0 \\ \vdots \\ (20\log_{10}\delta_p)^{M_p}(20\log_{10}\delta_s)^{M_s} \end{bmatrix}. \quad (16)$$

By fixing the value of f_c , denoted as $f_{c,1}$, and taking $4(M_p+1)(M_s+1)$ different sets of values of $N, \Delta B, \delta_p, \delta_s$ and $J(\delta_p, \delta_s, f_c, \Delta B, N)$, denoted as $N_k, \Delta B_k, \delta_{p,k}, \delta_{s,k}$ and $J_k(\delta_{p,k}, \delta_{s,k}, f_{c,1}, \Delta B_k, N_k)$ for $k = 1, 2, \dots, 4(M_p+1)(M_s+1)$, respectively, we have $4(M_p+1)(M_s+1)$ columns of $\mathbf{M}(N, \Delta B, \delta_p, \delta_s)$, denoted as $\mathbf{M}_k(N_k, \Delta B_k, \delta_{p,k}, \delta_{s,k})$. Denote

$$\begin{aligned} \hat{\mathbf{M}}(N, \Delta B, \delta_p, \delta_s) &= [\mathbf{M}_1(N_1, \Delta B_1, \delta_{p,1}, \delta_{s,1}), \dots, \\ &\dots, \mathbf{M}_{4(M_p+1)(M_s+1)}(N_{4(M_p+1)(M_s+1)}, \\ &\Delta B_{4(M_p+1)(M_s+1)}, \delta_{p,4(M_p+1)(M_s+1)}, \\ &\delta_{s,4(M_p+1)(M_s+1)}], \end{aligned} \quad (17)$$

$$\begin{aligned} J(\delta_p, \delta_s, f_c, \Delta B, N) &= [J(\delta_{p,1}, \delta_{s,1}, f_{c,1}, \Delta B_1, N_1) \dots \\ &J(\delta_{p,4(M_p+1)(M_s+1)}, \delta_{s,4(M_p+1)(M_s+1)}, f_{c,1}, \\ &\Delta B_{4(M_p+1)(M_s+1)}, N_{4(M_p+1)(M_s+1)})]^T. \end{aligned} \quad (18)$$

Suppose $\mathbf{M}_k(N_k, \Delta B_k, \delta_{p,k}, \delta_{s,k})$ for $k = 1, 2, \dots, 4(M_p+1)(M_s+1)$ are chosen in such a way that they are linearly independent, then $\hat{\mathbf{M}}(N, \Delta B, \delta_p, \delta_s)$ is invertible and

$$\begin{aligned} &(\hat{\mathbf{M}}(N, \Delta B, \delta_p, \delta_s))^{-1} 10\log_{10} J(\delta_p, \delta_s, f_{c,1}, \Delta B, N) \\ &= \hat{A}_f \sin(\hat{\omega}_f f_{c,1} + \phi_f) (\mathbf{a}). \end{aligned} \quad (19)$$

Similarly, by fixing the value of f_c to a different value, denoted as $f_{c,2}$, yields

$$\begin{aligned} &(\hat{\mathbf{M}}(N, \Delta B, \delta_p, \delta_s))^{-1} 10\log_{10} J(\delta_p, \delta_s, f_{c,2}, \Delta B, N) \\ &= \hat{A}_f \sin(\hat{\omega}_f f_{c,2} + \phi_f) (\mathbf{a}). \end{aligned} \quad (20)$$

Let the i -th element of the vectors \mathbf{a} , and $(\hat{\mathbf{M}}(N, \Delta B, \delta_p, \delta_s))^{-1} 10\log_{10} J(\delta_p, \delta_s, f_{c,\ell}, \Delta B, N)$ with $\ell = 1, 2$ be a_i and $v_{i,\ell}$ respectively. Then $v_{i,\ell} = (\hat{A}_f \sin(\hat{\omega}_f f_{c,\ell} + \phi_f) + 1)a_i$ for $i = 1, 2, \dots, 4(M_p+1)(M_s+1)$. This implies that

$$a_i = \frac{v_{i,\ell}}{\hat{A}_f \sin(\hat{\omega}_f f_{c,\ell} + \phi_f) + 1}, \quad (21)$$

and

$$\hat{A}_f = \frac{v_{i,2} - v_{i,1}}{v_{i,1} \sin(\hat{\omega}_f f_{c,2} + \phi_f) - v_{i,2} \sin(\hat{\omega}_f f_{c,1} + \phi_f)}. \quad (22)$$

A good estimate of \hat{A}_f and a_i can be obtained by

$$\begin{aligned} \bar{\hat{A}}_f &= \frac{1}{4(M_p+1)(M_s+1)} \times \\ &\sum_{i=1}^{4(M_p+1)(M_s+1)} \frac{v_{i,2} - v_{i,1}}{v_{i,1} \sin(\hat{\omega}_f f_{c,2} + \phi_f) - v_{i,2} \sin(\hat{\omega}_f f_{c,1} + \phi_f)}, \\ \bar{a}_i &= \frac{1}{2} \left(\frac{v_{i,1}}{\hat{A}_f \sin(\hat{\omega}_f f_{c,1} + \phi_f) + 1} + \frac{v_{i,2}}{\hat{A}_f \sin(\hat{\omega}_f f_{c,2} + \phi_f) + 1} \right), \end{aligned}$$

for $i = 1, 2, \dots, 4(M_p+1)(M_s+1)$.

4. DESIGN EXAMPLES

The application and accuracy of the presented empirical formula is best demonstrated by design examples, where various filter design parameters of the actual PCLS filter are compared with that estimated from the presented formula. The following simulations assume $W(\omega) = 1 \forall \omega \in B_p \cup B_s$ and a brickwall filter $D(\omega)$. First consider the estimation of the required filter length of the PCLS filter by considering the following design parameter set: $\delta_p = \delta_s = 0.01$, $f_c = \frac{\pi}{2}$ and $\Delta B = 0.08\pi$. Suppose that the target total ripple energy of the PCLS filter is -40 dB. Using $M_p = M_s = 5$, the proposed model requires 144 different sets of values of $N_k, \Delta B_k, \delta_{p,k}, \delta_{s,k}$ and $J_k(\delta_{p,k}, \delta_{s,k}, f_{c,1}, \Delta B_k, N_k)$ for $k = 1, 2, \dots, 144$, to estimate the model. These values are obtained by considering $\Delta B_k \in \{0.075\pi, 0.08\pi, 0.085\pi\}$, $\delta_{p,k} \in \{0.007, 0.009, 0.011, 0.013\}$, $\delta_{s,k} \in \{0.007, 0.009, 0.011, 0.013\}$ and $N_k \in \{28, 30, 32\}$. Then the PCLS filters are designed via solving the corresponding optimization problems defined in eq.(1) and eventually the corresponding values of $J_k(\delta_{p,k}, \delta_{s,k}, f_{c,1}, \Delta B_k, N_k)$ for $k = 1, 2, \dots, 144$ are obtained. As these values are obtained, the parameters of the model could be estimated by the method discussed in Section 3.6. By putting these estimated parameters as well as the specification values into the proposed model, the minimum filter length N required to meet the above design specification is found to be no less than 28. To verify the accuracy of the proposed model, PCLS filters with filter lengths $N = 26$ and $N = 28$ are designed subject to the same set of specifications ($\delta_p = \delta_s = 0.01, f_c = \frac{\pi}{2}$ and $\Delta B = 0.08\pi$). Fig 4(a) (for $N = 26$) and Fig 4(b) (for $N = 28$) show the magnitude response of the designed PCLS filters. It can be seen from Fig 4(a) that the stopband ripple magnitudes of the designed filter are all equal, so it is a minimax filter. The maximum passband ripple magnitude is equal to 0.0102, the maximum stopband ripple magnitude is equal to 0.0101 and the total ripple energy is equal to -38.7157 dB, which does not meet the required specification. On the other hand, it can be seen from Fig. 4(b) that the stopband ripple magnitudes of the designed filter are not all equal, so it is not a minimax filter. The maximum passband ripple magnitude is equal to 0.01, the maximum stopband ripple magnitude is equal to 0.0099 and the total ripple energy is equal to -44.2808 dB. Hence, the required specification is satisfied and the target total ripple energy is met. This implies that the minimum filter length required to meet the specification is $N = 28$, which is the same as predicted by the proposed model.

Another example considers the estimation of the transition bandwidth. The design parameters are given as $\delta_p = \delta_s = 0.006, f_c = \frac{\pi}{2}$ and $N = 32$. Suppose that the target total ripple energy of the PCLS filter is -45 dB. Based on the estimated parameters obtained in the first example, the minimum transition bandwidth is estimated to be $\Delta B = 0.08\pi$. PCLS filters with transition bandwidths equal to $\Delta B = 0.07\pi, 0.08\pi$ are designed subject to the same set of specifications. The magnitude responses of the design PCLS filters are shown in Fig 5(a) (for $\Delta B = 0.07\pi$) and Fig 5(b) (for $\Delta B = 0.08\pi$). It can be seen from Fig 5(a) that the maximum passband ripple magnitude is equal to 0.0079, the maximum stopband ripple magnitude is equal to 0.0075, and the total ripple energy is equal to -41.3010 dB, in which the required specification is not satisfied. On the other hand, it can be observed from Fig 5(b) that the

maximum passband ripple magnitude is equal to 0.006 , the maximum stopband ripple magnitude is equal to 0.0059 and the total ripple energy is equal to -49.4528dB . Hence, the required specification is satisfied and the target total ripple energy is met. This implies that the minimum transition bandwidth required to meet the specification is $\Delta B = 0.08\pi$, which is the same as that predicted by the proposed model.

5. CONCLUSIONS

The main contribution of this brief is to propose an empirical formula that relates the filter length, the transition bandwidth, the cut-off frequency, the maximum passband ripple magnitude, the maximum stopband ripple magnitude and the total ripple energy of symmetric/anti-symmetric FIR single band PCLS filters which is useful for defining the design specifications for PCLS filter for a given performance.

6. ACKNOWLEDGMENT

The work obtained in this brief was supported by a research grant from the Center for Multimedia Signal Processing (under project BB9D), The Hong Kong Polytechnic University.

REFERENCES

- [1] Charlotte Yuk-Fan Ho, Bingo Wing-Kuen Ling, Yan-Qun Liu, Peter Kwong-Shun Tam and Kok-Lay Teo, "Efficient algorithm for solving semi-infinite programming problems and their applications to nonuniform filter bank designs," *IEEE Transactions on Signal Processing*, vol.54, pp.4223-4232, Nov. 2006.
- [2] Ying-Man Law and Chi-Wah Kok, "Constrained eigenfilter design without specified transition bands," *IEEE Transactions on Circuits and Systems.II: Express Briefs*, vol.52, pp.14-21, Jan. 2005.
- [3] Samit Basu and Yoram Bresler, "An empirical study of minimax-optimal fractional delays for low-pass signals, *IEEE Transactions on Circuits and Systems.II: Analog and Digital Signal Processing*, vol. 49, no. 4, pp. 288-292, 2002.
- [4] Koichi Ichige, Mamoru Iwaki and Rokuya Ishii, "Accurate estimation of minimum filter length for optimum FIR digital filters," *IEEE Transactions on Circuits and Systems.II: Analog and Digital Signal Processing*, vol.47, pp.1008-1016, Oct. 2000.
- [5] John W. Adams, "FIR digital filters with least-squares stopbands subject to peak-gain constraints," *IEEE Transactions on Circuits and Systems*, vol.39, pp.376-388, April 1991.

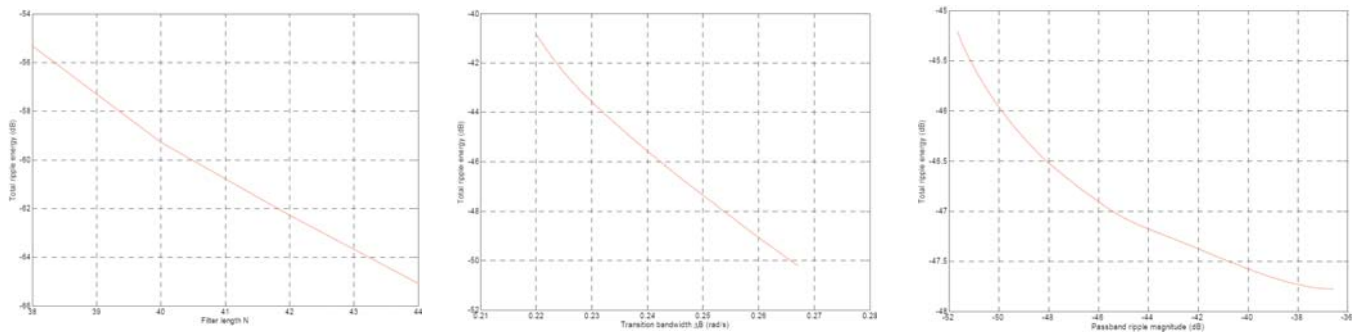


Figure 1: (a) Total ripple energy vs filter length; (b) Total ripple energy vs transition bandwidth; (c) Total ripple energy vs maximum passband ripple magnitude of a PCLS filter.

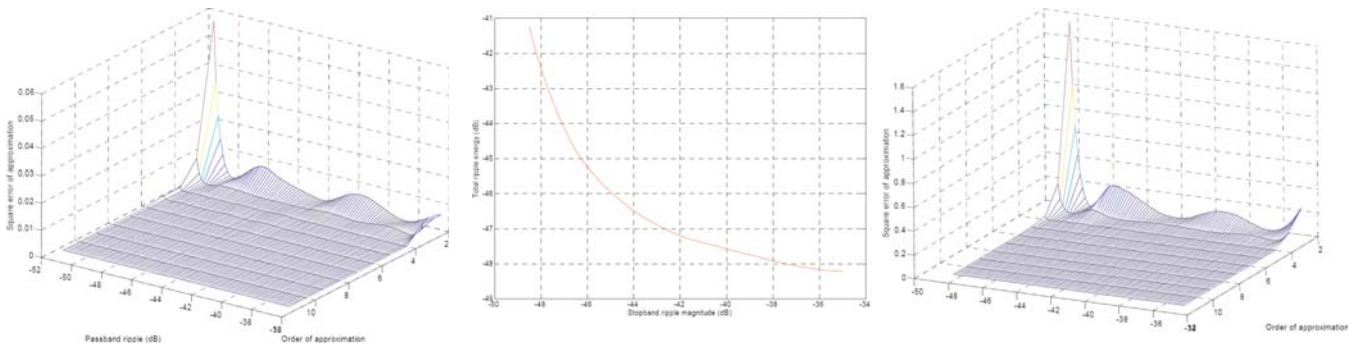


Figure 2: (a) $E_p(\delta_p, M_p)$ vs M_p and δ_p ; Total ripple energy vs maximum stopband ripple magnitude; $E_s(\delta_s, M_s)$ vs M_s and δ_s of a PCLS filter.

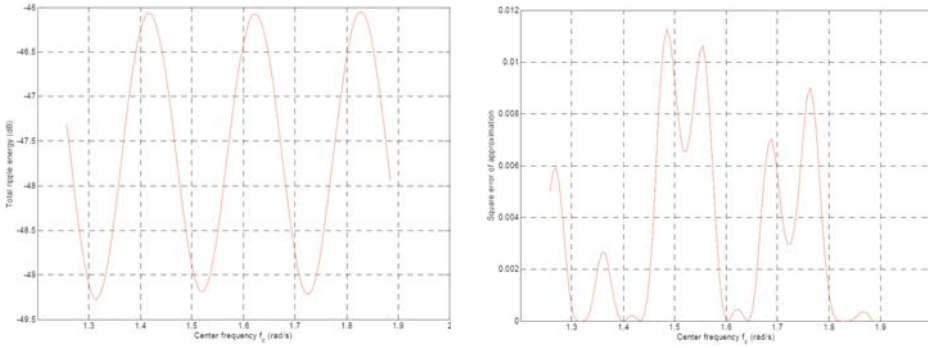


Figure 3: (a) Total ripple energy vs center frequency; (b) $E_f(f_c)$ vs f_c of a PCLS filter.

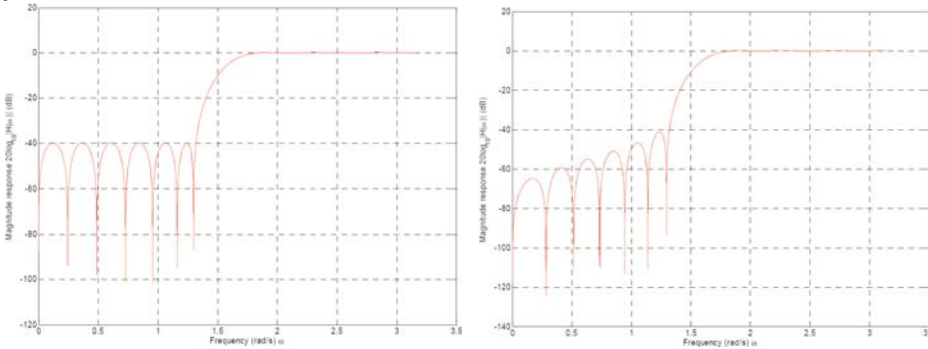


Figure 4: (a) Magnitude response of PCLS filter with $N = 26$; (b) Magnitude response of PCLS filter with $N = 28$.

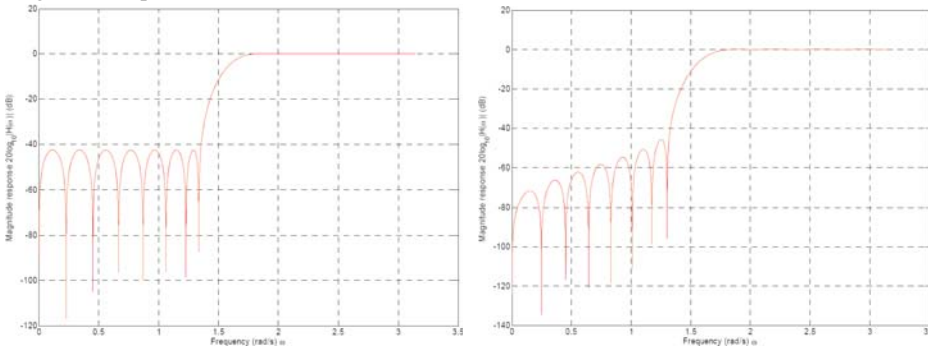


Figure 5: (a) Magnitude response of PCLS filter with $\Delta B = 0.07\pi$; (b) Magnitude response of PCLS filter with $\Delta B = 0.08\pi$.